

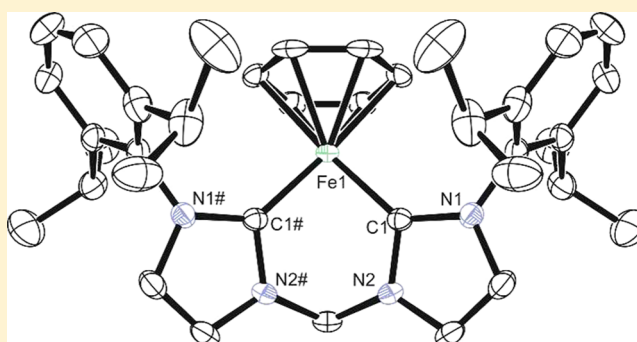
Bis-*N*-Heterocyclic Carbene (NHC) Stabilized η^6 -Arene Iron(0) Complexes: Synthesis, Structure, Reactivity, and Catalytic Activity

Burgert Blom, Gengwen Tan, Stephan Enthaler, Shigeyoshi Inoue, Jan Dirk Epping, and Matthias Driess*

Department of Chemistry: Metalorganics and Inorganic Materials, Technische Universität Berlin, Strasse des 17. Juni 135, Sekr. C2, D-10623 Berlin, Germany

Supporting Information

ABSTRACT: Reaction of FeCl_2 with the chelating bis-*N*-heterocyclic carbene (NHC) bis-(*N*-Dipp-imidazole-2-ylidene)methylene (abbreviated $\{(\text{DippC:})_2\text{CH}_2\}$ (Dipp = 2,6-di-isopropylphenyl) affords the complex $[\text{FeCl}_2\{(\text{DippC:})_2\text{CH}_2\}]$ (**1**) in high yield. Reduction of complex **1** with excess KC_8 with a 10-fold molar excess of PMe_3 affords the Fe(II) complex $[\text{FeH}\{(\text{DippC:})_2\text{CH}_2\}(\text{PMe}_3)(\eta^2\text{-PMe}_2\text{CH}_2)]$ (**2**) as a mixture of three stereoisomers. Complex **2**, the first example of any iron(II) complex bearing mutually an NHC and PMe_3 ligand, is likely obtained from the *in situ*, reductively generated 16 VE Fe(0) complex, $[\text{Fe}\{(\text{DippC:})_2\text{CH}_2\}(\text{PMe}_3)_2]$ (**2'**), following intramolecular C–H activation of one of the phosphorus-bound CH_3 groups.



Complex **2** is unstable in aromatic solvents and forms, *via* a novel synthetic transformation involving intramolecular reductive elimination and concomitant PMe_3 elimination, the Fe(0) arene complex $[\text{Fe}\{(\text{DippC:})_2\text{CH}_2\}(\eta^6\text{-C}_6\text{D}_6)]$ (**4-d₆**) in C_6D_6 . Complex **4-d₆** represents the first example of an NHC stabilized iron(0) arene complex. The transformation from **2** to **4-d₆** can be accelerated at higher temperature and at 60 °C forms immediately. Alternatively, the reduction of **1** in the presence of toluene or benzene affords the complexes $[\text{Fe}\{(\text{DippC:})_2\text{CH}_2\}(\eta^6\text{-C}_7\text{H}_8)]$ (**3**) and $[\text{Fe}\{(\text{DippC:})_2\text{CH}_2\}(\eta^6\text{-C}_6\text{H}_6)]$ (**4**), selectively and in good yields. DFT calculations characterizing the bonding situation in **3** and **4** reveal similar energies of the HOMO and LUMO orbitals, with the LUMO orbital of both complexes located on the Dipp rings of the bis-NHC. The HOMO orbital reflects a π -back-bonding interaction between the Fe(0) center and the chelating NHC ligand, while the HOMO-1 is associated with the arene interaction with the Fe(0) site. The calculations do not suggest any noninnocence of the coordinated arene in either complex. Moreover, the ^{57}Fe Mössbauer spectrum of **4** at 80 K exhibits parameters ($\delta = 0.43 \text{ mm}\cdot\text{s}^{-1}$; $\Delta E_Q = 1.37 \text{ mm}\cdot\text{s}^{-1}$) which are consistent with a five-coordinate Fe(0) system, rendering **3** and **4** the first examples of well-defined authentic Fe(0)- η^6 -arene complexes of the type $[\text{Fe}(\eta^6\text{-arene})\text{L}_2]$ ($\text{L} = \eta^1$ or η^2 neutral ligand, mono or bidentate). Some reactivity studies of **3** are also reported: The reaction of **3** with excess CO selectively yields the five-coordinate piano-stool complex $[\text{Fe}\{(\text{DippC:})_2\text{CH}_2\}(\text{CO})_3]$ (**6**) in near quantitative yields, while the reaction of complex **3** with C_6D_6 under heating affords by toluene elimination **4-d₆**. The catalytic ability of **4** was also investigated with respect to amide reduction to amines, for a variety of substrates using Ph_2SiH_2 as a hydride source. In all cases good to excellent yields to the corresponding amines were obtained. The use of **4** as a precatalyst represents the first example of a well-defined Fe(0) complex to effect this catalytic process.

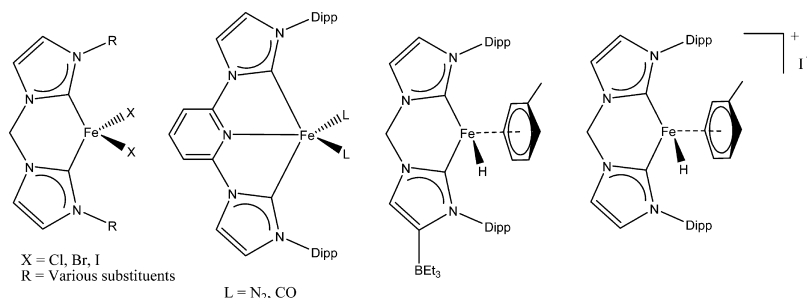
INTRODUCTION

The landmark discovery of an isolable *N*-heterocyclic carbene (NHC) by Arduengo and co-workers in 1991¹ heralded a paradigm shift in contemporary coordination and organometallic chemistry. NHC ligands typically exhibit enhanced σ -donor capacity and concomitant increased robustness when compared to traditional phosphine complexes, which has encouraged their remarkable development and particular interest as supporting ligands in catalysis.² In recent years iron-based NHC complexes, with a particular focus on catalytic applications, have received considerable attention owing to the high natural abundance and low cost of the element.³ Highlights within the last two years include the selective reduction of esters to aldehydes using $[\text{Fe}^0(\text{CO})_4(\text{NHC})]$ as

precatalyst,⁴ catalytic arene borylation using the complex $[\text{Cp}^*\text{Fe}(\text{NHC})(\text{R})]$ ($\text{R} = \text{alkyl group}$),⁵ or the recently reported hydrosilylation of imines, mediated by an NHC iron catalyst, all highlighting the potential of these complexes.⁶

Chelating bis-NHC ligands have also recently been shown to be rather versatile in accessing some interesting Fe complexes: the simultaneous reports of Meyer and co-workers⁷ and Ingleson and co-workers⁸ have for example shown that complexes of the type $[\text{FeL}_2\text{X}_2]$ ($\text{X} = \text{Cl or Br}$, $\text{L}_2 = \text{chelating bis(imidazolylidene) ligand}$) are readily accessible upon reaction of $[\text{Fe}\{\text{N}(\text{SiMe}_3)_2\}_2]$ as an Fe(II) source with

Received: August 6, 2013

Chart 1. Some Recent Examples of Chelating NHC Stabilized Iron Complexes^{7–9,11}

bis(imidazolium) chloride or bromide salts. The emerging complexes were shown to be tetrahedral high-spin iron(II) complexes on the basis of structural studies and Mössbauer investigations. Saßmannshausen and Motherwell reported the synthesis of pincer-type pyridyl bis-NHC complexes of the type $[\text{Fe}(\text{C}-\text{N}-\text{C})(\text{N}_2)_2]$ accessible by reduction of the corresponding dihalides under a N₂ atmosphere.⁹ Very recently, intriguing four-coordinate Fe(II) complexes have also been reported by Chen and co-workers by reaction of *in situ* generated silver bis(pyridylimidazolylidene)methane adducts with elemental iron, directly.¹⁰ Finally, several Fe(II) hydride complexes have also been reported, supported by chelating bis-NHC ligands (Chart 1).¹¹ These recent examples highlight the active research area into which Fe-based NHC chemistry is flourishing.

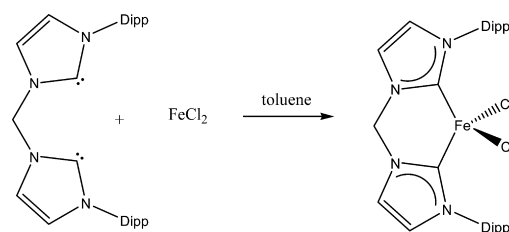
We initially became interested in exploring the use of the NHC bis-(*N*-Dipp-imidazole-2-ylidene)methylene, abbreviated $\{(\text{DippC:})_2\text{CH}_2\}$ (Dipp = 2,6-di-isopropylphenyl),¹² as a supporting ligand for main group element compounds in low-oxidation states.¹³ Given our concurrent interest in low-valent iron complexes and their chemistry, particularly with respect to new catalytic precursors,¹⁴ we became interested in trying to obtain iron(0) complexes with this supporting ligand, which might act as a source of the “L₂Fe(0)” fragment, if bearing additional stabilizing ligands, capable of elimination.¹⁵ We reasoned that using PMe₃ as additional stabilizing ligands could enable access to 16 VE complexes of the type $[\text{L}_2\text{Fe}(\text{PMe}_3)_2]$ (L₂ = $\{(\text{DippC:})_2\text{CH}_2\}$), which would be excellent sources of Fe(0) by concomitant PMe₃ elimination.¹⁶ Alternatively, η^6 -arene complexes could be accessible upon reduction of $[\text{L}_2\text{FeCl}_2]$ in the presence of arenes, affording complexes of the type $[\text{Fe}\{(\text{DippC:})_2\text{CH}_2\}(\eta^6\text{-arene})]$, as these 18 VE closed-shell complexes should be stable. Surprisingly, such complexes have escaped isolation, and we felt warranted investigation.¹⁷

By using the chelating bis-NHC ligand $\{(\text{DippC:})_2\text{CH}_2\}$, we report the first examples of Fe(0) η^6 -arene complexes stabilized exclusively by NHCs. Moreover an example of an Fe^{II} bis-phosphane complex featuring $\{(\text{DippC:})_2\text{CH}_2\}$ as a supporting ligand, which is the first example of an iron(II) complex bearing a PMe₃ and NHC ligand mutually, is also discussed. In addition, the reactivity of one of the Fe(0) $\{(\text{DippC:})_2\text{CH}_2\}$ -(η^6 -arene) complexes is reported, along with the first catalytic investigations of organic amide reduction, starting from a well-defined Fe(0) complex: $[\text{Fe}\{(\text{DippC:})_2\text{CH}_2\}(\eta^6\text{-C}_6\text{H}_6)]$

RESULTS AND DISCUSSION

We first synthesized the precursor $[\text{FeCl}_2\{(\text{DippC:})_2\text{CH}_2\}]$ (**1**) by reaction of the free bis-NHC ligand with anhydrous FeCl₂ in toluene, which afforded a beige solid after workup in high

yields. Characterization of **1** (Scheme 1) was severely impeded by its insolubility in hydrocarbon solvents, a problem which has

Scheme 1. Synthesis of **1** by Coordination of $\{(\text{DippC:})_2\text{CH}_2\}$ to FeCl₂

1: beige paramagnetic solid, 81 %

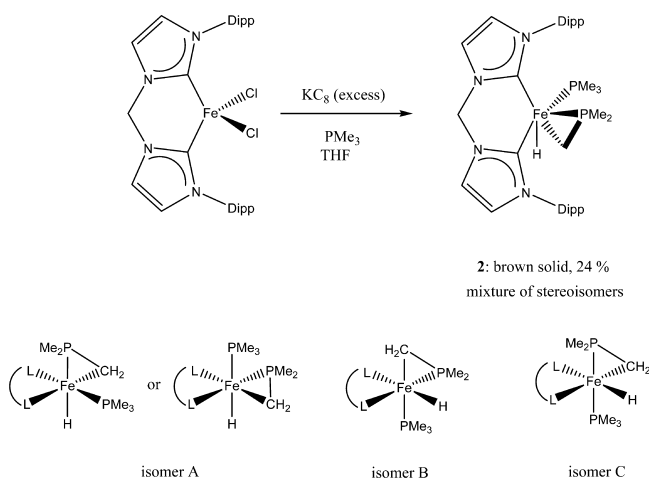
been remarked on before, in the literature, for similar complexes by Ingleson and Meyer, respectively.^{7,8} It is noteworthy to mention that this synthetic route to **1** differs from the earlier approach by Meyer and Ingleson to access analogous complexes, who both employed the reaction of $[\text{Fe}\{\text{N}(\text{SiMe}_3)_2\}_2]$ with bis(imidazolium) dihalide salts affording the desired complexes. Simple coordination of the free bis-NHC as ligand to FeCl₂ appears to be an alternative route to access these complexes. The ¹H NMR spectrum of **1** reveals a highly paramagnetic substance which is consistent with the analogous examples by Meyer and Ingleson.^{7,8} Numerous attempts to obtain crystals suitable for X-ray diffraction analysis of **1** were unsuccessful owing to the insolubility of the complex in a variety of solvents, and its instability for prolonged periods in CH₂Cl₂. However, the composition on the basis of both EIMS and HRMS was confirmed, and a ⁵⁷Fe Mössbauer spectrum was also recorded at 80 K ($\delta = 0.69 \text{ mm}\cdot\text{s}^{-1}$; $\Delta E_Q = 3.67 \text{ mm}\cdot\text{s}^{-1}$). The latter reveal parameters which are comparable to the complexes of Meyer which lie in the range $\delta = 0.73\text{--}0.81 \text{ mm}\cdot\text{s}^{-1}$; $\Delta E_Q = 3.67\text{--}4.03 \text{ mm}\cdot\text{s}^{-1}$. These values are typical of high-spin Fe(II) complexes (*S* = 2) in a tetrahedral environment, further confirming the identity of **1**.

With the availability of **1**, we next targeted the 16 VE complex, $[\text{Fe}\{(\text{DippC:})_2\text{CH}_2\}(\text{PMe}_3)_2]$ (**2'**) by reduction of **1** with excess KC₈ in THF with an excess of PMe₃ (10 molar equiv). The initial phase of the reaction has the appearance of a beige suspension, which slowly turns brown upon stirring. Workup afforded a hexane soluble fraction, which when crystallized, according to NMR, was not the desired product (**2'**) but the hydrido Fe(II) complex, $[\text{FeH}\{(\text{DippC:})_2\text{CH}_2\}(\text{PMe}_3)(\eta^2\text{-PMe}_2\text{CH}_2)]$ (**2**). Complex **2** is surprisingly the first example of any iron(II) complex featuring an NHC and PMe₃ ligand mutually coordinated to the iron center.^{18,19} It seems reasonable that the desired **2'** was generated as an initial

reduction product *in situ*, but subsequently, due to the electronically and coordinatively unsaturated iron center, induced an intramolecular C–H activation of one of the phosphorus-bound methyl groups. A similar process occurs on reducing $[\text{FeCl}_2(\text{PMe}_3)_2]$ in the presence of excess PMe_3 , affording the C–H activated six-coordinate complex, $[\text{FeH}(\text{PMe}_3)_3(\eta^2\text{-PMe}_2\text{CH}_2)]$.²⁰

The ^1H and $^{31}\text{P}\{^1\text{H}\}$ NMR spectra of **2** in benzene- d_6 at room temperature revealed an extraordinarily complex pattern, consistent with the coexistence of three stereoisomers (Scheme 2).²¹ This is exemplified by three resonance bands in the

Scheme 2. Reduction of 1 in the Presence of Excess PMe_3 , Affording 2 as a Mixture of Stereoisomers^a



^aThe reaction most likely proceeds *via* the electron-poor 16VE intermediate $[\text{Fe}\{(\text{DippC})_2\text{CH}_2\}(\text{PMe}_3)_2]$ (**2'**), which then undergoes C–H activation affording **2**. ($\text{L-L} = \{(\text{DippC})_2\text{CH}_2\}$).

hydride region of the ^1H NMR spectrum, each of which exhibits a doublet of doublet (dd) multiplicity corresponding to $^2J(\text{H},\text{P}_a)$ and $^2J(\text{H},\text{P}_b)$ coupling for each stereoisomer respectively (Figure 1). The $^1\text{H}\{^{31}\text{P}\}$ spectrum reveals only three single lines in the hydride region corresponding to each of the stereoisomers (Figure 1). Moreover, 12 resonance signals are observed for the methine protons $\text{CH}(\text{CH}_3)_2$ of the Dipp substituents, which correspond to four diastereotopic groups for each stereoisomer. This can be expected by the loss of symmetry afforded by the geometric structures of isomers A to C. There is no indication of any interconversion between the three stereoisomers, as all the signals are very sharp, and a static distribution of these stereoisomers is observed in the ratio of 40:28:32 (A:B:C). The $^{31}\text{P}\{^1\text{H}\}$ NMR spectrum reveals a similar static picture: three sets of signals (each set featuring two doublet resonance signals: one high-field shifted, corresponding the $\eta^2\text{-PMe}_2\text{CH}_2$ ligand and one low-field shifted for the Fe-PMe_3 for each stereoisomer. Moreover, a two-dimensional (^1H , ^{31}P) correlation spectrum enabled assignment of the hydride signals to the corresponding signal sets in the $^{31}\text{P}\{^1\text{H}\}$ NMR spectrum. On the basis of coupling constants (H,P and P,P), together with the two-dimensional NMR spectra, a tentative assignment of the isomers could be made, where for isomer A there are two geometric possibilities which could not unambiguously be distinguished from each other (Scheme 2).

It is apparent from these spectra that on the respective time scale of the measurements,²² no interconversion or exchange process is occurring between the three stereoisomers, and a static picture is revealed. Strikingly, on the time scale of the corresponding $^{13}\text{C}\{^1\text{H}\}$ NMR measurement, a surprisingly highly symmetric spectrum is observed, at odds with those in the ^1H and ^{31}P spectra, featuring sharp signals assignable to only one component, as opposed to three observed in the ^1H and ^{31}P spectra (Figure 2).²³ Further investigations revealed that the spectrum originates from the $\text{Fe}(0)$ arene complex

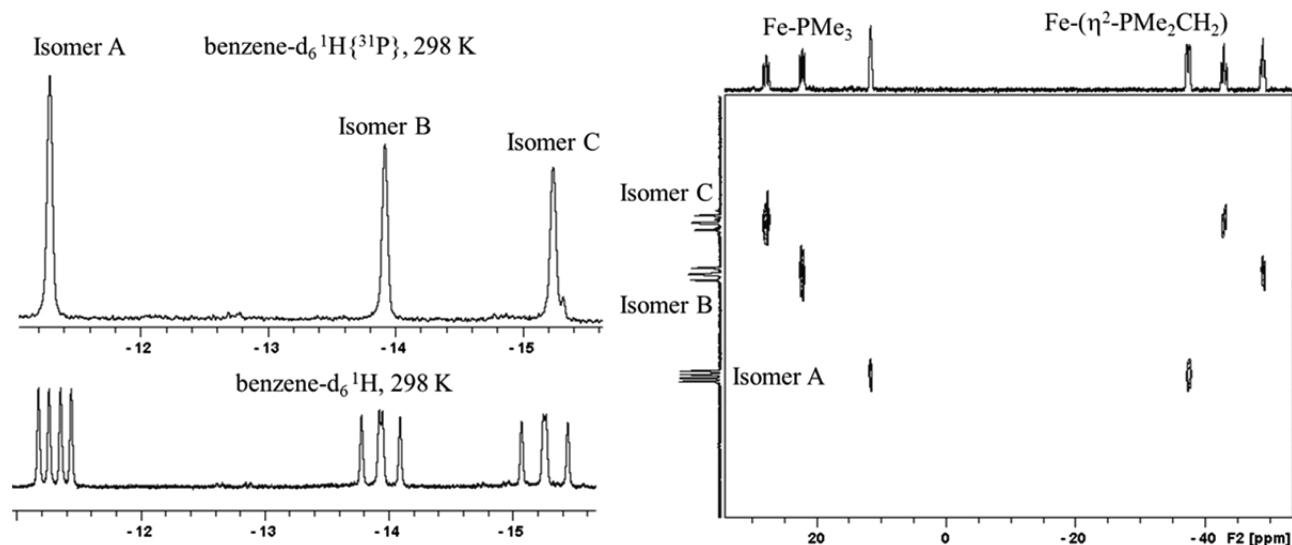


Figure 1. ^1H NMR spectrum in benzene- d_6 at 298 K in the hydride region of **2** (left, bottom) showing three distinct resonance signals with dd multiplicities; isomer C: $^2J(\text{H},\text{P}_a) = 69.6$ Hz, $^2J(\text{H},\text{P}_b) = 81.2$ Hz; isomer B: $^2J(\text{H},\text{P}_a) = 57.7$ Hz, $^2J(\text{H},\text{P}_b) = 68.2$ Hz; isomer A: $^2J(\text{H},\text{P}_a) = 34.7$ Hz, $^2J(\text{H},\text{P}_b) = 71.9$ Hz, and the corresponding $^1\text{H}\{^{31}\text{P}\}$ spectrum (left, top). Two dimensional (^1H , ^{31}P) NMR spectrum in benzene- d_6 at 298 K of **2** showing correlation of hydride resonance signals to respective doublet signals (right, top). $\delta = -48.2$ (d, $^2J(\text{P}_a,\text{P}_b) = 46.3$ Hz, isomer B), $\delta = -42.1$ (ps d, $^2J(\text{P}_a,\text{P}_b) = 56.1$ Hz, isomer C), $\delta = -36.7$ (d, $^2J(\text{P}_a,\text{P}_b) = 27.5$ Hz, isomer A), $\delta = 12.5$ (d, $^2J(\text{P}_a,\text{P}_b) = 27.5$ Hz, isomer A), $\delta = 23.0$ (d, $^2J(\text{P}_a,\text{P}_b) = 46.3$ Hz, isomer B), $\delta = 28.5$ (ps d, $^2J(\text{P}_a,\text{P}_b) = 56.1$ Hz, isomer C).

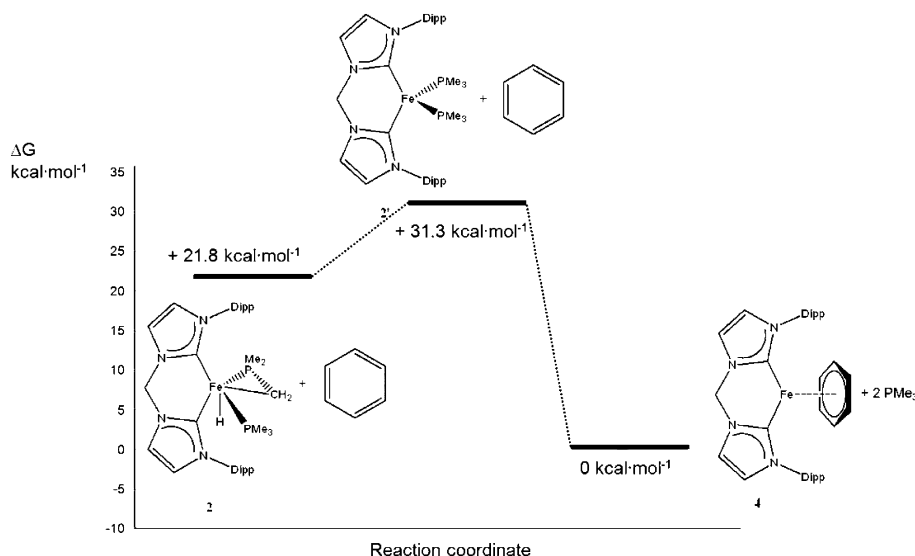
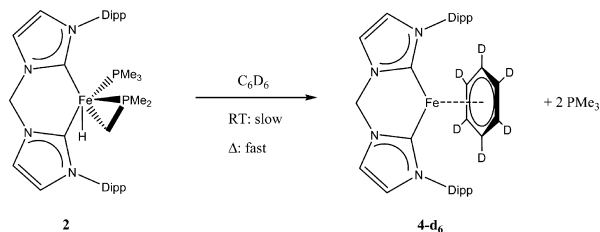


Figure 2. DFT (B3LYP/6-31G* for all atoms) calculated energies on transformation of **2** to **4** via **2'**.

[Fe{(DippC:)₂CH₂}(η⁶-C₆D₆)] (**4-d₆**) which is formed spontaneously from **2** by PMe₃ loss (presumably involving an initial intramolecular reductive elimination step first forming **2'**) and concomitant coordination of the solvent (C₆D₆). We uncovered **4-d₆** as the product by comparing the spectrum to the authentic spectra of **4-d₆** obtained by other means (see below) and by comparison to the nondeuterated analogue, **4**. Complex **2** is hence unstable for prolonged periods of time in C₆D₆, and given the time required for recording the ¹³C NMR spectrum (several hours), clean conversion from **2** to **4-d₆** at room temperature is observed in this time period. A key resonance signal in the ¹³C NMR spectrum of **4-d₆** is that of the η⁶-C₆D₆ ring at *d* = 75.2 ppm as a triplet due to ¹J(C,D) = 24.9 Hz coupling. Hence, complex **4-d₆** represents the first example of an NHC stabilized Fe(0) arene complex, obtained fortuitously on standing for prolonged periods in C₆D₆ from **2**.

The conversion of **2** to **4-d₆** was additionally investigated by VT NMR experiments of **2** where immediate conversion to **4-d₆** is observed at or above 320 K (Scheme 3, see Supporting Information).

Scheme 3. Transformation of 2 to the Fe(0) Arene Complex 4-d₆ in C₆D₆ by Concomitant PMe₃ Elimination



A DEPT-135 spectrum (with an acquisition time of no more than 0.5 h) of a very concentrated sample of **2** in C₆D₆ indeed reveals a very complex spectrum, corresponding to the signals for the stereoisomeric mixture of **2**, before the onset of the slow, room temperature conversion to the highly symmetric spectrum corresponding to **4-d₆**. Additionally, heating a sample of **2** in a nonaromatic solvent (for example hexane) results in decomposition, which suggests that the arene is necessary to stabilize the emerging Fe(0) complex resulting from the PMe₃

elimination. These results show that **2** can be employed as a starting material to access novel Fe(0) arene complexes in a facile manner.

Based on these findings, the mechanism accompanying this novel transformation is likely intramolecular reductive elimination in **2** affording the transient 16 VE species [Fe{(DippC:)₂CH₂}(PMe₃)₂] (**2'**), which is subsequently trapped by the 6 VE donor arene ligand, with PMe₃ elimination. The selective formation of **4-d₆** as the only product resulting from **2** is more convincing evidence of the presence of the stereoisomeric mixture in **2** all of which converge by the process described above to **4-d₆**.

This novel transformation from **2** to **4-d₆** was also elucidated by DFT methods using the nondeuterated analogue (**4**) (B3LYP/6-31G* for all atoms) (Figure 2). In accordance with our experimental observations, the process is spontaneous with the energies of **2** + C₆H₆ being 21.8 kcal·mol⁻¹ higher than that of **4** + 2 PMe₃, inferring an exergonic process. The likely intermediate **2'** + C₆H₆ exhibits an energy of 31.3 kcal·mol⁻¹, and this increase in energy also explains why the reduction of **1** in the presence of PMe₃ affords **2** and not **2'**, as the latter is slightly higher in energy and less thermodynamically stable. The transition states between each step in the transformation were not located (Figure 2), and so a discussion on the energy barriers is neglected.

The solid-state structure of one of the stereoisomers of **2** was also determined by single crystal X-ray diffraction analysis and is shown in Figure 3, along with some key metric parameters (a figure showing the coordination geometry at iron is also presented in Figure 3b, where the Dipp groups have been removed for clarity).

The solid-state structure of **2** corresponds structurally to the previously discussed isomer C, bearing two nearly transpositioned phosphine groups. Some disorder is located on the P2 atom, which could be resolved, and is omitted from the structural representation in Figure 3 and the following discussion. The complex can be considered distorted octahedral, with the hydride hydrogen atom residing in the pocket formed by the atoms C37, P, C1, and P1. The presence of a strained three-membered P2, C37, Fe1 ring along with the small size of the H atom can account for this distorted

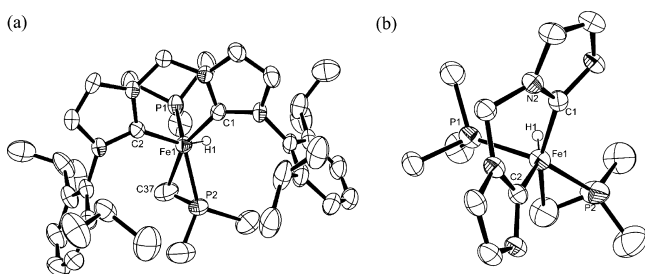


Figure 3. (a) ORTEP representations of the solid-state structure of one of the stereoisomers of **2** at the 50% probability level. H atoms, except that of the Fe–H site (H1), were omitted for clarity. (b) View of **2** where the Dipp groups and all H atoms (except H1) were omitted for clarity. Selected bond lengths [Å] and angles [°]: Fe1–C1 1.915(3), Fe1–C2 1.919(3), Fe1–C37 2.086(9), Fe1–P1 2.1693(11), Fe1–P2 2.152(3); C1–Fe1–C2 90.10(14), C1–Fe1–C37 158.9(3), C2–Fe1–C37 105.7(4), C1–Fe1–P2 116.44(13), C2–Fe1–P2 117.69(14), C37–Fe1–P2 43.7(3), C1–Fe1–P1 99.21(10), C2–Fe1–P1 98.15(10), C37–Fe1–P1 92.5(4), P2–Fe1–P1 127.57(13).

octahedral structure. Noteworthy are the Fe1–C1 (1.915(3) Å) and Fe1–C2 bond lengths (1.919(3) Å) which are considerably shorter in comparison to those found for example in the four-coordinate Fe(II) complex L_2FeCl_2 (L = methylenebis-(*N*-benzyl-imidazole-2-ylidene)methylene by Meyer and co-workers at 2.107(3) and 2.111(3) Å, respectively.⁷ This bond length contraction can be accounted for by increased π -back-donation from the Fe(II) center in **2**, to the carbene carbon atoms, facilitated by the presence of electron pushing alkyl phosphane ligands in the coordination sphere. The bond lengths are comparable in magnitude but still slightly shorter to those found in the Fe(II) η^6 arene complex by Ingleson, $[Fe\{^{Dipp}C\}_2CH_2]H(\eta^6\text{-toluene})$, at 1.952(3) and 1.951(3) Å, respectively.¹¹

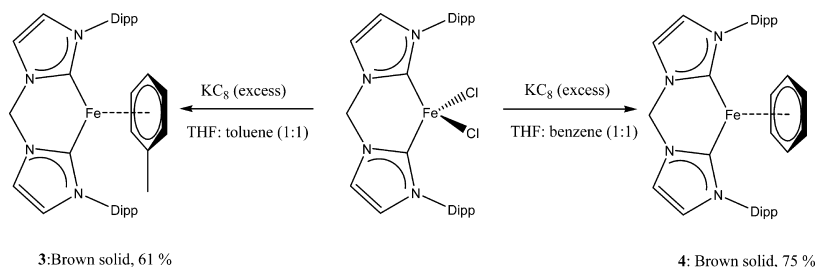
The inaccessibility of the desired 16 VE Fe(0) precursor by the strategy detailed above, which instead afforded us an Fe(II) complex, shown subsequently to undergo facile PMe_3 elimination forming the NHC stabilized Fe(0) arene complex, prompted us to explore the reduction of **1** in the presence of aromatic solvents to directly afford the NHC stabilized Fe(0) arene complexes. To our surprise such complexes have not been reported (with the exception of **4-d₆**), although perusal of the literature in fact states access to such complexes are not possible, starting from the di-iodo analogue of **1**, $[FeI_2\{^{Dipp}C\}_2CH_2]$. Moreover, it is also stated that reduction of $[FeI_2\{^{Dipp}C\}_2CH_2]$ in the presence of several other trapping agents also does not yield the desired Fe(0) complexes.¹¹

However, we observed that reduction of **1** in 1:1 (v/v) THF:arene (toluene or benzene) mixtures with excess KC_8

cleanly and in good yields afforded the desired bis-NHC Fe(0) arene complexes **3** and **4** as dark brown, highly air sensitive solids (Scheme 4). It was found essential to add THF to the reaction since the precursor **1** is insoluble in toluene or benzene, and the THF was required to slightly solubilize the starting material for the reaction to occur (Scheme 4).

Complexes **3** and **4** are remarkable since they are (other than **4-d₆**) the first examples of Fe(0) arene complexes supported exclusively by NHC ligands. This is even more surprising, when one considers the fact that complexes of the type $[Fe(\eta^6\text{-arene})(PR_3)_2]$ (R = halogen, alkyl, or aryl substituent) have existed since 1972.²⁴ Despite their early entry in the literature, these complexes have escaped characterization by structural methods, probably as a result of their extreme reactivity, or the fact that they are liquids at ambient temperature.²⁵ Moreover access to these complexes typically require complicated metal vapor synthetic techniques, making their access somewhat difficult.²⁶ The related and somewhat more robust arene complexes by Girolami and co-workers bearing a chelating phosphane ligand, $[P_2Fe(\eta^6\text{-arene})]$ (P_2 = chelating bidentate phosphane ligand), have been known for more than 15 years but have also escaped structural characterization,²⁷ while the related complex $[P_2Fe(\eta^6\text{-naphthalene})]$, reported by Komiya and co-workers has been structurally studied.²⁸ This complex was claimed to be Fe(0), but no theoretical or Mössbauer studies were carried out to prove this, and it was subsequently shown by Wolf and co-workers that naphthalene has the propensity to behave in a noninnocent fashion in a variety of low-valent iron complexes, drawing the assignment of the oxidation state of iron in $[P_2Fe(\eta^6\text{-naphthalene})]$ into question.²⁹ Chirik and co-workers have reported complexes of the type $[L'2Fe(\eta^6\text{-arene})]$ where L' = bis imine in 2005, but again the redox noninnocence of the bis-imine was firmly established.³⁰ Finally, even as early as 1982 Klabunde and co-workers reported the synthesis of $[(2,2'\text{-bipyridine})Fe(\eta^6\text{-toluene})]$, purported to be an Fe(0) complex with substantial π -back-bonding from the Fe(0) center to the Bipy ligand.³¹ This description of the bonding situation was however subsequently shown to be incorrect on the basis of theoretical calculations by Wieghardt and Scarborough.³² The complex rather exists as a singlet diradical where the Fe(I) (d^7 , $S_{Fe} = 1/2$) center couples antiferromagnetically to the redox noninnocent bipy radical anion ($bipy^{\bullet-}$). This renders the strikingly facile isolation of complexes **3** and **4** an important entry in the context of Fe η^6 -arene complexes, given this historical background; especially in light of the redox innocence afforded by the chelating NHC ligand. The redox innocence of the NHC ligands moreover, in fact, renders them the first examples of well-defined authentic Fe(0) arene complexes of the type $[Fe(\eta^6\text{-arene})L_2]$ ³³ on the basis of the simultaneous analyses of

Scheme 4. Facile Synthesis of the Unprecedented Fe(0) Arene Complexes **3** and **4**



structural, DFT methods, Mössbauer studies, and spectroscopy, which all corroborate this fact (*vide infra*).

The ^1H NMR spectra of **3** and **4** exhibit no resonance signals in the negative chemical shift region (hydride region), so any Fe–H species, like those reported by Ingleson (Chart 1), can be ruled out. The ^1H NMR spectrum of **3** exhibits a highly symmetric pattern in agreement with expectations for the structure of **3**. Noteworthy, the ^1H NMR spectrum of **4** is identical to that of the deuterated analogue, **4-*d*₆**, except for an additional signal for the coordinated arene, which is not seen in the deuterated case (see Supporting Information). Moreover, the signal for the coordinated arene in **4** shows up as a singlet in the ^{13}C spectrum, compared to a triplet for the case of **4-*d*₆**, due to C,D coupling in the latter case, but both are virtually at the same chemical shift.

Additionally, the $^{13}\text{C}\{^1\text{H}\}$ NMR spectra of both complexes feature sharp lines and spectra reflecting high symmetry indicative of free rotation of the arene ligands, in analogy to the observations in the ^1H NMR spectra. Noteworthy is the presence of only one resonance signal corresponding to both carbene carbon atoms (NC:N), around $\delta = 200$ ppm, which is the expected position for this resonance. In complex **3**, in accordance with the ^1H , ^{13}C correlation spectra, three aromatic carbon resonance signals corresponding to C^{2,6}, C^{3,5} and C⁴ for the coordinated toluene ring were observed, along with the corresponding three resonance bands in the ^1H spectrum (Figure 4). The C¹ signal of the toluene is also observable at $\delta = 77.9$ ppm.

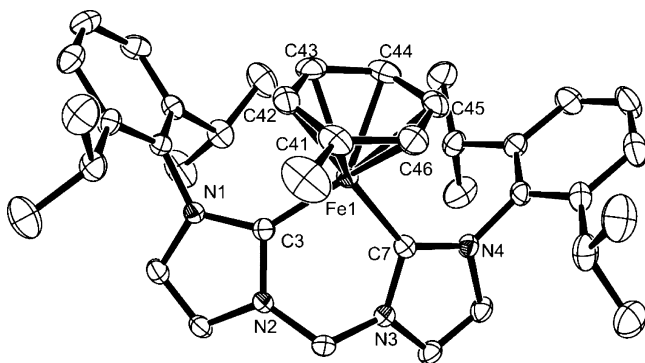


Figure 4. ORTEP representation of **3**·Et₂O in the solid state at 50% probability. H atoms omitted for clarity, in addition to the cocrystallized Et₂O molecule. Selected bond lengths [Å]: Fe1–C3 1.9190(19), Fe1–C7 1.9212(19), Fe1–C42 2.096(2), Fe1–C41 2.096(2), Fe1–C43 2.107(2), Fe1–C46 2.114(2), Fe1–C44 2.118(2), Fe1–C45 2.135(2), C41–C46 1.409(3), C41–C42 1.422(3), C42–C43 1.410(3), C43–C44 1.407(3), C44–C45 1.413(3), C45–C46 1.406(3). Selected bond angle [°]: C3–Fe–C7 89.36(8).

The $^{13}\text{C}\{^1\text{H}\}$ NMR spectra for **3** and **4** also exhibit a resonance signal at $\delta \sim 60$ ppm corresponding to the methylene group bridging the two NHC moieties, although in **4**, this signal could only be located in the HMQC spectrum. Moreover, in both complexes, two resonance signals corresponding to the CH=CH backbone of the NHC, i.e., C^AH=C^BH and C^AH=C^BH, respectively, is observed and could be assigned on the basis of the HMQC spectrum.

Complexes **3** and **4** were also elucidated structurally by single crystal X-ray diffraction analysis investigations. Crystals of **3** were grown from a saturated Et₂O solution with slow cooling,

while those of **4** were grown from a benzene/Et₂O solution with careful cooling to 5 °C. Figures 4, 5, and 6 show the solid-state structures of **3** and **4**, respectively, with some key metric parameters in each case. Complex **3** has a cocrystallized Et₂O molecule in the asymmetric unit.

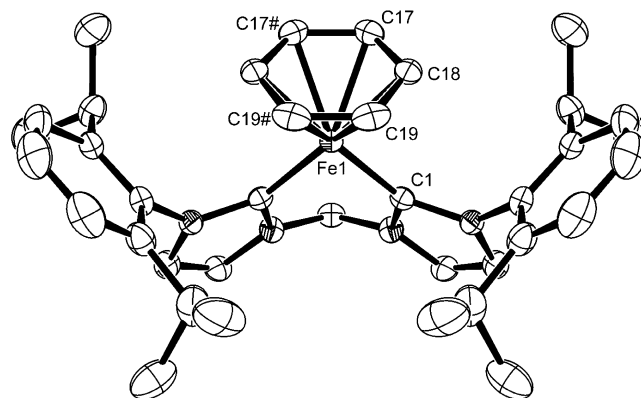


Figure 5. ORTEP representation of **4** in the solid state at 50% probability. H atoms omitted for clarity. (Symmetry transformations used to generate equivalent atoms #: 1 – *x* + 2, *y*, *z*). Selected bond lengths [Å]: Fe1–C1 1.921(3), Fe1–C19 2.119(3), Fe1–C17 2.121(3), Fe1–C18 2.125(3), C17–C17# 1.404(6), C17–C18 1.405(4), C18–C19 1.416(5), C19–C19# 1.385(7). Selected bond angle [°]: C1–Fe1–C1# 88.92(16).

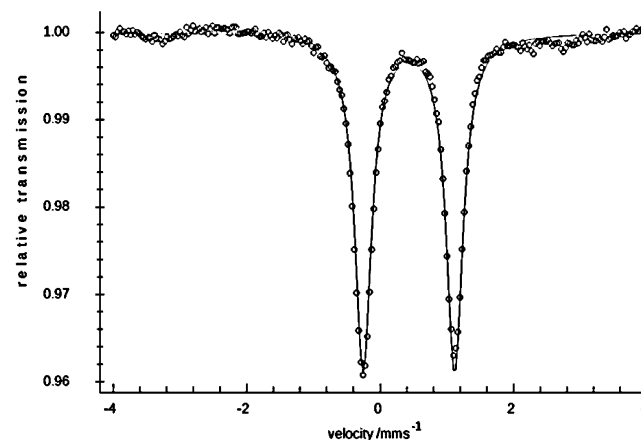


Figure 6. ^{57}Fe Mössbauer spectrum of complex **4** in the solid state at 80 K. Circles are the experimental data, lines the simulated data. A small amount of a background impurity is present, most likely degradation products, evidenced by a small aberration in the baseline of the collected data. Parameters for **4**: $\delta = 0.43$ mm·s^{–1}; $\Delta E_Q = 1.37$ mm·s^{–1}.

Both complexes **3** and **4** exhibit very similar structural features in the solid state and are both “two-legged piano-stool” complexes. Complexes **3** and **4** can alternatively be thought of as exhibiting pseudotrigonal bipyramidal geometry, if one considers the arene to occupy three coordination sites at the iron center. This idea is particularly attractive, since the bite angle of the chelating NHC is 89.36(8) in **3** and 88.92(16) in **4**, respectively, so it can be thought of as occupying the remaining two sites of the trigonal bipyramid. The structure of **4** exists in the *Cmc*2₁ space group and possesses symmetry rendering the one-half of the molecule metrically invariant to the other half. The Fe to NHC bond distances in both complexes is comparable (**3**: 1.9190(19) Å, 1.9212(19) Å; **4**: 1.921(3) Å,

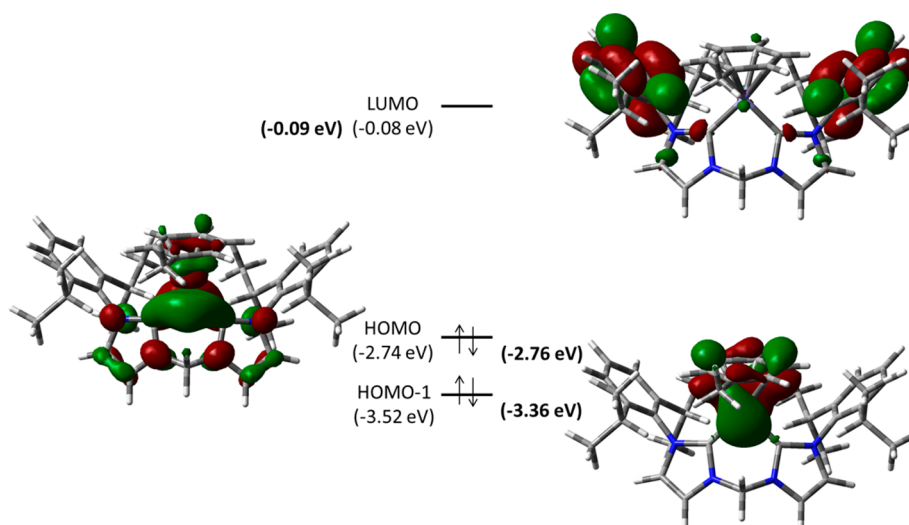
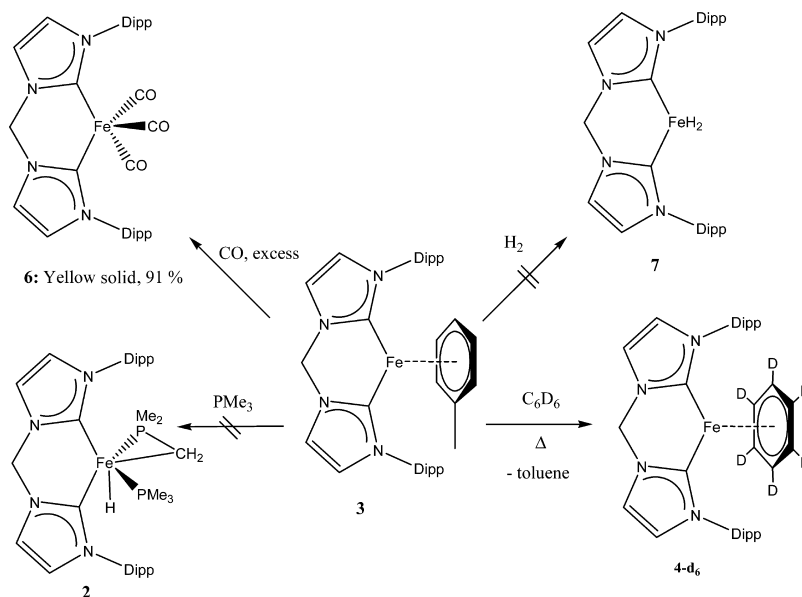


Figure 7. Boundary surfaces of the calculated frontier molecular orbitals in complex **3**. The energies in bold parentheses are the calculated energies for the corresponding MOs in complex **4** which are comparable.

Scheme 5. Preliminary Reactivity Studies of Fe(0) Arene Complex **3**



respectively) and surprisingly comparable to those found in **2**, despite the reduced oxidation state of the metal. The iron to NHC bond distances, in **3** and **4**, are however shorter in comparison to the four coordinate Fe(II) complex L_2FeCl_2 (L = methylenebis-(*N*-benzyl-imidazole-2-ylidene) by Meyer and co-workers at 2.107(3) and 2.111(3) Å, respectively.⁷ This bond length contraction suggests π -back-bonding from the electron-rich Fe(0) center to the carbene carbon atoms. This is certainly a novel feature of these complexes compared with the existing $L_2Fe(\eta^6\text{-arene})$ (L_2 = bis-imine or phosphine) complexes so far reported, which bear ligands not capable of π -acceptance from Fe or possess noninnocent ligands (see Theoretical Calculations section for further discussion). The bond distances between the iron and carbon atoms of the arene ring in **3** are comparable to each other within narrow limits, and the same can be said for that of **4**, indicative of η^6 -arene coordination to the iron centers in both complexes. There is no indication of reduction in the arene rings on the basis of their

associated metric parameters, in both complexes, which indeed do suggest their redox innocence.

Complex **4** was additionally analyzed by ^{57}Fe Mössbauer spectroscopy at 80 K in the solid state, to determine its oxidation state and additionally rule out any possible “non-innocence” of the η^6 -arene. The spectrum is presented in Figure 6.

Although some ^{57}Fe Mössbauer spectroscopic studies have been reported for well-defined five coordinate Fe(0) complexes,³⁴ their interpretation is somewhat more difficult than for Fe(II) complexes, which typically are approximately octahedral symmetric.³⁵ A recent systematic study has however been carried out for five-coordinate Fe(0) complexes of the type $[P_2FeL]^n$ (P = chelating bis-phosphane ligand; L = PMe_3 , N_2 , $SnCl(2,6\text{-}Mes_2\text{-}C_6H_3)$; $E(2,6\text{-}Mes_2\text{-}C_6H_3)^+$ (E = Ge, Sn); $Ge(2,6\text{-}Trip_2\text{-}C_6H_3)^+$),³⁶ where it was shown that these complexes, exhibit isomer shift values in the range $\delta = 0.17\text{--}0.43\text{ mm}\cdot\text{s}^{-1}$. Moreover, the ΔE_Q parameter, for this series, fluctuates strongly depending on whether a trigonal bipyramidal

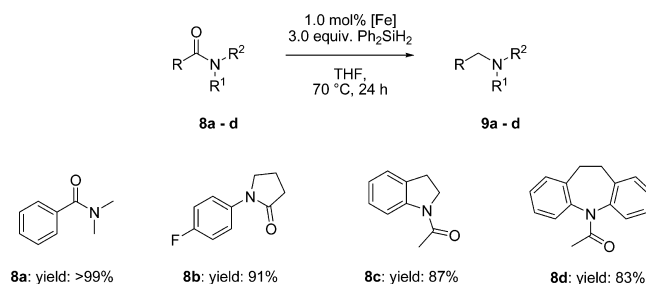
The reaction of **3** with CO at 1 atm pressure results in an almost immediate color change to bright yellow with concomitant arene elimination and formation of **6**. Complex **6** has been reported before as a “major product” resulting from the reaction of $[\text{Fe}\{(\text{D}^{\text{ipp}}\text{C})_2\text{CH}_2\}(\text{H})(\text{HBET}_3)]\cdot\text{LiI}$ with excess CO, but only IR data and an X-ray structure are reported, and no further spectroscopic or other compositional data are

provided.¹¹ Moreover, the authors claim the complex is “unstable” in vacuo and even stated that decomposition occurs in solution under an N₂ atmosphere resulting in an intractable mixture. The fate of the iron-bound hydride, LiH, and HBEt₃ is unclear, although BEt₃ is said to be generated during the reaction, according to NMR data, along with H₂. Using **3** as an alternate starting material, complex **6** is isolable in near quantitative yields, by clean toluene elimination at iron. Moreover, in our hands, complex **6** was found to be rather robust and no decomposition was observed after drying in vacuo for 0.5 h. We also found complex **6** to be stable in solutions under N₂ for long periods of time, evidenced by the long NMR measuring time (overnight) which afforded reasonable spectra. The ¹H and ¹³C{¹H} NMR spectra of **6** are in accordance with expectations, and a full assignment could be made. A key feature in the ¹³C{¹H} NMR spectrum in **6** is a single resonance signal at $\delta = 223$ ppm corresponding to the three equivalent CO ligands, pointing to a rather symmetric structure. The rather robust nature of the complex is further highlighted by the ESI-MS spectrum where, in fact, the three fragmentations corresponding to [M + H]⁺, [M – CO + H]⁺, [M – 2CO + H]⁺, and [M – 3 CO + H]⁺ (the three decarbonylation steps) are all visible with fitting isotope distribution patterns in each case. Our recorded IR spectrum of isolated **6** in benzene $\nu(\text{CO}, \text{cm}^{-1})$: 1968, 1890, 1865, moreover matches that reported by Ingleson: (THF solution) $\nu(\text{CO}, \text{cm}^{-1})$: 1968, 1891, 1864. This is typical for carbonyl complexes of the type *cis*-L₂M(CO)₃, with local C_s symmetry at the metal center, with 2A' and 1A'' IR active modes, in accordance with expectations for **6**.

Catalytic Reduction of Organic Amides with Complex

4. Iron-based catalysis now enjoys considerable attention as alternatives to traditional catalysts based to a large extent on precious and toxic metals (e.g., Rh, Ir, Ru, Pd, Pt) owing to its great abundance, low cost, and low toxicity.⁴¹ Recently, excellent performances with iron-based precatalysts have been demonstrated in the reduction chemistry of a variety of organic substrates. Inspired by this fact we were interested in exploring the catalytic abilities of complex **4**. We targeted the reduction of organic amides to form amines, particularly since no investigations have been reported on well-defined iron(0) complexes for such transformations and, in fact for the most part, are limited to *in situ* generated iron(II) systems.⁴² In the presence of catalytic amounts of complex **4** (1.0 mol %), a number of organic amides bearing different steric and electronic properties were converted, in good to excellent yields to the corresponding tertiary amines applying Ph_2SiH_2 as a hydridosilane source, under mild reaction conditions (Scheme 6). Noteworthy, these results are comparable, or even superior

Scheme 6. Catalytic Application of Complex 4 in the Reduction of Organic Amides to Amines



in some cases, to some modern benchmark systems for other iron-based amide reduction systems. The advantage of using complex **4** is that the starting point is a well-defined precatalyst which could certainly facilitate facile mechanistic studies of the mechanism associated with this reductive process, and is currently under investigation.

CONCLUSION

Unprecedented Fe(0) NHC stabilized η^6 -arene complexes have been reported using a facile synthetic route involving reduction of $[\text{FeCl}_2\{(\text{DippC})_2\text{CH}_2\}]$ (**1**), bearing a chelating NHC, in the presence of toluene or benzene. These complexes, surprisingly, are the first examples of well-defined (on the basis of structural, DFT, spectroscopic, and Mössbauer studies) genuine Fe(0) arene complexes of the type $[\text{Fe}(\eta^6\text{-arene})\text{L}_2]$ ($\text{L} = \eta^1$ or η^2 neutral ligand, mono or bidentate), rendering them somewhat remarkable. Moreover, the first example of an iron(II) complex featuring a PMe_3 and NHC ligand at the iron center also stabilized by the chelating NHC $\{(\text{DippC})_2\text{CH}_2\}$ has also been accessed in a similar fashion and likely forms by way of a 16 VE complex, $[\text{Fe}(\text{PMe}_3)_2\{(\text{DippC})_2\text{CH}_2\}]$ (**2'**). This complex was also shown to undergo facile PMe_3 elimination and provides an alternative and novel route Fe(0) arene complexes. The arene complexes have been demonstrated to be good precursors for further chemistry, exemplified, inter alia, by the reaction of $[\text{Fe}\{(\text{DippC})_2\text{CH}_2\}(\eta^6\text{-C}_7\text{H}_8)]$ (**3**) with CO affording $[\text{Fe}\{(\text{DippC})_2\text{CH}_2\}(\text{CO})_3]$ (**6**) selectively, by arene elimination. Arene exchange (toluene/benzene) was found to only occur upon heating, due to the close energies of the frontier orbitals in **3** and **4**. In addition, the first catalytic investigations of organic amide reduction, starting from a well-defined Fe(0) precursor were undertaken with $[\text{Fe}\{(\text{DippC})_2\text{CH}_2\}(\eta^6\text{-C}_6\text{H}_6)]$ (**4**) which afforded good to excellent conversions in all cases to the corresponding amines. We are currently exploring the reduction of $[\text{FeCl}_2\{(\text{DippC})_2\text{CH}_2\}]$ (**1**) in the presence of a broad range of trapping agents to target highly reactive electron-deficient Fe(0) complexes and shall report these endeavors in due course.

EXPERIMENTAL SECTION

All experiments and manipulations were carried out under dry oxygen-free nitrogen using standard Schlenk techniques or in an MBraun inert atmosphere glovebox containing an atmosphere of purified nitrogen. Hexane, diethylether, benzene, and toluene and THF were dried by standard methods and additionally stirred over LiAlH_4 , after which they were recondensed and degassed at least once prior to use. Benzene- d_6 was stirred over KC_8 for a period of 48 h and then degassed, followed by recondensing it into a bulb containing activated 4 Å mol sieves, where it was stored. Cyclohexane- d_{12} and dichloromethane- d_2 were syringed into vessels containing freshly activated 4 Å mol sieves and stored for several weeks to complete the removal of trace water. Both solvents were subsequently degassed by a freeze–pump–thaw cycle prior to use. The bis-carbene ligand bis-(*N*-Dipp-imidazole-2-ylidene)methylene $\{(\text{DippC})_2\text{CH}_2\}$ (Dipp = 2,6-diisopropylphenyl) was prepared according to literature procedure.¹² The NMR spectra were recorded on a Bruker AV 200 or 400 Spectrometer. Concentrated solutions of samples in benzene- d_6 /cyclohexane- d_{12} /dichloromethane- d_2 were sealed off in a Young-type NMR tube for measurements. The ^1H and $^{13}\text{C}\{^1\text{H}\}$ were referenced to the residual solvent signals as internal standards ($\delta_{\text{H}} = 7.15$; $\delta_{\text{C}} = 128.0$ ppm for benzene- d_6 ; $\delta_{\text{H}} = 1.38$; $\delta_{\text{C}} = 26.4$ ppm cyclohexane- d_{12} ; $\delta_{\text{H}} = 5.32$ dichloromethane- d_2). $^{31}\text{P}\{^1\text{H}\}$ spectra were externally calibrated with H_3PO_4 in sealed capillaries. Abbreviations: s = singlet; m = multiplet; br = broad, sept = septet. In the case of broad signals, half-height widths (HHW, $\Delta\nu_{1/2}$) are quoted in Hz. Unambiguous signal

assignments were made by employing a combination of 2D NMR ^1H -COSY and ^1H -C-COSY (HMQC, HMBC) experiments and additional to DEPT experiments as required. High-resolution ESI mass spectra were recorded on an Orbitrap LTQ XL of Thermo Scientific mass spectrometer, and the raw data evaluated using the X-calibur computer program. In each case the line of highest intensity is reported in the isotope pattern. For the single crystal X-ray structure analyses the crystals were each mounted on a glass capillary in perfluorinated oil and measured in a cold N_2 flow. The data of compounds **2**–**4** were recorded on an Oxford Diffraction Supernova, single source at offset, atlas at 150 K (Cu- $\text{K}\alpha$ -radiation, $\lambda = 1.5418$ Å). The structures were solved by direct methods and refined on F^2 with the SHELX-97 software package. The positions of the H atoms were calculated and considered isotropically according to a riding model, and in the case of **2** the position of the hydride atom was constrained. The ^{57}Fe Mössbauer spectrum of **4** was recorded at the Max-Planck-Institute for Chemical Energy Conversion (CEC) on a spectrometer with alternating constant acceleration. The sample temperature was maintained in an Oxford Instruments Variox cryostat. The γ source was ~ 0.6 GBq $^{57}\text{Co}/\text{Rh}$. The quoted isomer shifts are relative to Fe metal at 300 K. The zero-field splitting spectrum was simulated by using Lorentzian doublets.

Synthesis of $[\text{FeCl}_2\{(\text{DippC})_2\text{CH}_2\}]$ (1**).** Anhydrous FeCl_2 (0.135 g, 1.065 mmol) and 'free' ligand bis-(*N*-Dipp-imidazole-2-ylidene)-methylene (0.500 g, 1.067 mmol) was added to a Schlenk tube in the glovebox. Toluene (50 mL) was added under rapid stirring to this mixture *via* cannula at room temperature. A brownish suspension results. The reaction was stirred overnight at room temperature after which it was concentrated to ~ 10 mL. Removal of the light-brown supernatant liquid *via* cannula afforded a beige solid, which was dried in vacuo at room temperature for several hours. Yield: 0.516 g (0.866 mmol, 81%). (The complex is insoluble in THF, toluene, benzene, acetonitrile, and only sparingly soluble in dichloromethane, but in the latter solvent slowly decomposes to a brown product over time. As a result of this insolubility, purification by crystallization is impossible. Attempts at growing crystals were also unsuccessful owing to the poor solubility.) ^1H NMR (200.13 MHz, dichloromethane- d_2 , 298 K): $\delta = -9.04$ (v br), -7.40 (v br), -3.14 (v br, $\Delta\nu_{1/2} = 195$ Hz), -1.49 (v br, $\Delta\nu_{1/2} = 51.6$ Hz), 1.23 (v br, $\Delta\nu_{1/2} = 45.5$ Hz), 2.32 (v br, $\Delta\nu_{1/2} = 30.7$ Hz), 6.43 (v br, $\Delta\nu_{1/2} = 51.3$ Hz), 7.18 (v br, $\Delta\nu_{1/2} = 46.8$ Hz), 24.33 (v br, $\Delta\nu_{1/2} = 186.6$ Hz), 58.80 (v br, $\Delta\nu_{1/2} = 80.4$ Hz). Elemental analysis calcd (%) for $\text{C}_{31}\text{H}_{40}\text{Cl}_2\text{FeN}_4$: C 62.53, H 6.77, N 9.47; found: C 61.26, H 6.95, N 9.07. EI-MS (70 eV), m/z : 594 (M^+ , 10%), 579 ($[\text{M} - \text{CH}_3]^+$, 8%), 559 ($[\text{M} - \text{Cl}]^+$, 5%), 454 (9%), 411 (12%), 228 ($[\text{DippC}]^+$, 68%). HRMS (EI), m/z : calcd for $\text{C}_{31}\text{H}_{40}\text{Cl}_2\text{FeN}_4$: 594.19740. Found: 594.19798 (1.0 ppm deviation). HR-ESI in THF yielded no signals due to poor insolubility. ^{57}Fe Mössbauer 80 K: $\delta = 0.69$ mm·s $^{-1}$; $\Delta E_{\text{Q}} = 3.67$ mm·s $^{-1}$.

$[\text{FeH}\{(\text{DippC})_2\text{CH}_2\}(\text{PMe}_3)(\eta^2\text{-PMe}_2\text{CH}_2)]$ (2**).** A Schlenk tube was charged with **1** (0.250 g, 0.417 mmol) and an excess of KC_8 (0.153 g, 1.132 mmol) and place in a -30 °C bath and the two solids stirred rapidly. A THF solution containing a 10-fold molar excess of PMe_3 was added to this mixture at low temperature (-30 °C) *via* cannula. The reaction mixture was allowed to warm to room temperature within 0.5 h and stirred for a further 5 h at room temperature. After 5 h an intense red color is observed. All volatiles were removed under reduced pressure affording a red-brown residue, which was then extracted with hexane at room temperature (60 mL). The filtrate (red-brown) was concentrated in vacuo to ~ 1 mL affording a brown solid which was isolated by decantation of the mother liquor. The resulting brown solid was dried in vacuo at room temperature for 0.5 h. Yield: 0.067 g (0.099 mmol, 24%). (Some cocrystallized hexane is present in the sample and is omitted from the data below.) Crystals suitable for single crystal X-ray diffraction analysis were grown from a concentrated Et_2O solution at -30 °C. ^1H NMR (200.13 MHz, benzene- d_6 , 298K): $\delta = -15.26$ (dd, $^2J(\text{H,P}_a) = 69.6$ Hz, $^2J(\text{H,P}_b) = 81.2$ Hz, $1 \times \text{Fe-H}$, isomer C, 32% abundance), -13.95 (dd, $^2J(\text{H,P}_a) = 57.7$ Hz, $^2J(\text{H,P}_b) = 68.2$ Hz, $1 \times \text{Fe-H}$, isomer B, 28% abundance), -11.33 (dd, $^2J(\text{H,P}_a) = 34.7$ Hz, $^2J(\text{H,P}_b) = 71.9$ Hz, $1 \times \text{Fe-H}$, isomer A, 40% abundance), -2.26 – -1.91 (m, Fe- CH_2 , isomer A), -1.53 –

−0.95 (m, Fe-CH₂, isomer B + C), 0.55–1.60 (m, Fe-P(CH₃)₃ + Fe-P(CH₃)₂ + CH(CH₃)(CH₃'), isomers A, B, and C), 2.43 (sept, ³J(H,H) = 6.8 Hz, CH^A(CH₃)(CH₃)), 2.64 (sept, ³J(H,H) = 7.4 Hz, CH^B(CH₃)(CH₃)), 2.79 (ps sept, ³J(H,H) = 6.5 Hz, CH^{C+D}(CH₃)(CH₃)), 3.05 (ps sept, ³J(H,H) = 6.7 Hz, CH^{E+F}(CH₃)(CH₃)), 3.38 (ps sept, ³J(H,H) = 7.1 Hz, CH^{G+H+I+J}(CH₃)(CH₃)), 3.58 (sept, ³J(H,H) = 7.5 Hz, CH^K(CH₃)(CH₃)), 4.00 (sept, ³J(H,H) = 7.1 Hz, CH^L(CH₃)(CH₃)), 4.39–5.28 (m, NCH₂N, isomers A + B + C), 6.16–6.64 (m, CH=CH, isomers A + B + C), 6.94–7.70 (m, ArH, isomers A + B + C). ¹H NMR (400.13 MHz, benzene-*d*₆, 298 K): δ = −15.26 (dd, ²J(H,P_a) = 69.6 Hz, ²J(H,P_b) = 81.2 Hz, 1 × Fe-H, isomer C, 32% abundance), −13.95 (dd, ²J(H,P_a) = 57.7 Hz, ²J(H,P_b) = 68.2 Hz, 1 × Fe-H, isomer B, 28% abundance), −11.33 (dd, ²J(H,P_a) = 34.7 Hz, ²J(H,P_b) = 71.9 Hz, 1 × Fe-H, isomer A, 40% abundance), −1.97 – −1.17 (m, Fe-CH₂, isomer A), −1.47 – −0.99 (m, Fe-CH₂, isomer B + C), 0.57 – 1.56 (m, Fe-P(CH₃)₃ + Fe-P(CH₃)₂ + CH(CH₃)(CH₃'), isomers A, B, and C), 2.33–2.50 (overlapping septs, CH^{A+B}(CH₃)(CH₃)), 2.65 (sept, ³J(H,H) = 6.9 Hz, CH^C(CH₃)(CH₃)), 2.80 (sept, ³J(H,H) = 6.7 Hz, CH^D(CH₃)(CH₃)), 2.99 (sept, ³J(H,H) = 6.7 Hz, CH^E(CH₃)(CH₃)), 3.07 (sept, ³J(H,H) = 6.7 Hz, CH^F(CH₃)(CH₃)), 3.31–3.45 (overlapping septs, CH^{G+H+I+J}(CH₃)(CH₃)), 3.58 (sept, ³J(H,H) = 6.8 Hz, CH^K(CH₃)(CH₃)), 4.02 (sept, ³J(H,H) = 7.1 Hz, CH^L(CH₃)(CH₃)), 4.40–5.26 (m, NCH₂N, isomers A + B + C), 6.16 – 6.64 (m, CH=CH, isomers A + B + C), 6.94–7.70 (m, ArH, isomers A + B + C). ¹H{³¹P} NMR (200.13 MHz, benzene-*d*₆, 298K): δ = −15.26 (s, 1 × Fe-H, isomer C) −13.95 (s, 1 × Fe-H, isomer B), −11.33 (s, 1 × Fe-H, isomer A) (all other resonance signals omitted). ³¹P{¹H} NMR (81.01 MHz, benzene-*d*₆, 298K): δ = −48.2 (d, ²J(P_aP_b) = 46.3 Hz, Fe-CH₂PMe₃, isomer B), δ = −42.1 (ps d, ²J(P_aP_b) = 56.1 Hz, Fe-CH₂PMe₃, isomer C), δ = −36.7 (d, ²J(P_aP_b) = 27.5 Hz, Fe-CH₂PMe₃, isomer A), δ = 12.5 (d, ²J(P_aP_b) = 27.5 Hz, Fe-PMe₃, isomer A), δ = 23.0 (d, ²J(P_aP_b) = 46.3 Hz, Fe-PMe₃, isomer B), δ = 28.5 (ps d, ²J(P_aP_b) = 56.1 Hz, Fe-PMe₃, isomer C). Recording a ¹³C{¹H} NMR spectrum of **2** with an acquisition time of ~6 h shows only **4-d**₆. DEPT 135 ¹³C{¹H} (100.61 MHz, benzene-*d*₆, 298 K, short acquisition time) shows a very complex pattern (see Supporting Information), consistent with several coexisting stereoisomers. ESI-MS (THF), *m/z*: calcd for [C₃₇H₃₈N₄P₂Fe]^{•+}: 676.3481. Found: 676.3508.

Thermal transformation of [FeH(D^{ipp}PC)₂(CH₂)₂(PMe₃)(η²-PMe₂CH₂)] (2**) to [Fe(D^{ipp}PC)₂(CH₂)₂(η⁶-C₆D₆)] (**4-d**₆).** A concentrated sample of isolated **2**-hexane was dissolved in C₆D₆ in a sealed NMR tube. A room temperature NMR spectrum revealed a spectrum consistent with **2** and small amounts of free PMe₃. The sample was slowly heated in the spectrometer and ¹H and ³¹P{¹H} NMR spectra recorded at *T* = 310, 320, and 330 K, respectively. Progressive liberation of PMe₃, concomitant collapse of the hydride signals of **2** at ~−11 to −15 ppm into the baseline, and selective formation of **4-d**₆ is observed in the ¹H NMR spectrum. Similarly, in the ³¹P{¹H} NMR spectrum, the three sets of doublet signals corresponding to the isomeric mixture of **2** collapse progressively into the baseline, with concomitant increase in the signal at δ = −63.3 ppm, corresponding to free PMe₃. (The spectra of **4-d**₆ are virtually identical to **4** (vide infra) except for the signals corresponding to the deuterated arene ring, see Supporting Information.) ¹H NMR (400.13 MHz, benzene-*d*₆, 298 K): δ = 0.79 (br s, 18 H, 2 × PMe₃ (free)), 1.05 (br d, ³J(H,H) = 6.2 Hz, 12 H, 2 × CH(CH₃)₂), 1.44 (br d, ³J(H,H) = 5.4 Hz, 12 H, 2 × CH(CH₃)₂), 3.41 (br m, 4 H, 4 × CH(CH₃)₂), 4.43 (br s, 2 H, 1 × NCH₂N), 6.19 (br s, 4 H, 2 × CH^A=CH^B), 6.90–7.40 (solvent signal + m, 6 H, Ar-H).

¹³C{¹H} NMR (101 MHz, benzene-*d*₆, 298 K): δ = 16.4 (m, free PMe₃), 23.1 (s, 2 × CH(CH₃)₂), 25.8 (s, 2 × CH(CH₃)₂), 28.6 (s, 4 × CH(CH₃)₂), 59.7 (s, 1 × NCH₂N), 75.5 (t, ¹J(C,D) = 24.9 Hz, 6 × CD, η⁶-C₆D₆), 116.3 (s, 2 × CH^A=CH^B), 123.0 (s, 2 × CH^A=CH^B), 124.1 (s, 2 × C^{3,5}-H, Dipp), 129.1 (s, 2 × C⁴-H, Dipp), 140.3 (s, 2 × C¹, Dipp), 147.7 (s, C^{2,6}, Dipp), 197.8 (s, 2 × NC:N). ³¹P{¹H} NMR (81.01 MHz, benzene-*d*₆, 298 K): δ = −63.3 (free PMe₃).

Removal of all volatiles from the NMR tube, followed by resolution in C₆D₆ affords **4-d**₆ (without PMe₃). ¹H NMR (400.13 MHz,

benzene-*d*₆, 298 K): δ = 1.05 (br d, ³J(H,H) = 6.2 Hz, 12 H, 2 × CH(CH₃)₂), 1.44 (br d, ³J(H,H) = 5.4 Hz, 12 H, 2 × CH(CH₃)₂), 3.41 (br m, 4 H, 4 × CH(CH₃)₂), 4.43 (br s, 2 H, 1 × NCH₂N), 6.19 (br s, 4 H, 2 × CH^A=CH^B), 6.90–7.40 (solvent signal + m, 6 H, Ar-H). ³¹P{¹H} NMR (81.01 MHz, benzene-*d*₆, 298K): silent.

[Fe(D^{ipp}PC)₂(CH₂)₂(η⁶-C₇H₈)] (3**).** A Schlenk tube was charged with **1** (0.141 g, 0.237 mmol) and an excess of KC₈ (0.081 g, 0.60 mmol). A 1:1 (by volume) THF/toluene solution was added with rapid stirring at room temperature to the solid mixture *via* cannula. The initial reaction appears as a beige suspension. The reaction was stirred at room temperature overnight during which the reaction appearance changed to a dark-brown solution. All volatiles were removed under reduced pressure, and the resulting brown residue extracted with hexane (60 mL). The brown filtrate was concentrated to 1 mL and allowed cooled to −30 °C overnight to complete crystallization. The mother liquor was subsequently decanted, and the remaining brown solid dried in vacuo at room temperature for 0.5 h affording a brown solid as product. Yield: 0.089 g (0.144 mmol, 61%). (The reaction can be scaled up, where we found that concentration of the reaction mixture to ~5 mL, followed by adding hexane, and then extraction, followed by workup provided the best yields. In this way the resulting dark-brown filtrate was pumped down affording an oily brown residue. Two freeze–pump–thaw cycles and scratching this residue into a powder was subsequent followed by resolution of the solid and “stripping” in Et₂O, with drying in vacuo for 0.5 h which affords **3**·OEt₂ as product). Crystals suitable for single crystal X-ray diffraction analysis were grown from a concentrated Et₂O solution at −30 °C. ¹H NMR (400.13 MHz, cyclohexane-*d*₁₂, 298 K): δ = 1.80 (br d, ³J(H,H) = 14.4 Hz, 24 H, 4 × CH(CH₃)₂), 2.74 (br s, Δν_{1/2} = 21.0 Hz, 3 H, 1 × CH₃, η⁶-toluene), 3.48 (br s, Δν_{1/2} = 26.2 Hz, 2 H, Ar-H, η⁶-toluene), 3.68 (br s, Δν_{1/2} = 71.8 Hz, 4 H, 4 × CH(CH₃)₂), 4.33 (br s, Δν_{1/2} = 25.1 Hz, 2 H, Ar-H, η⁶-toluene), 5.15 (br s, Δν_{1/2} = 44.1 Hz, 2 H, 1 × NCH₂N), 5.30 (br s, Δν_{1/2} = 32.4 Hz, 1 H, Ar-H, η⁶-toluene), 6.61 (br s, Δν_{1/2} = 22.3 Hz, 2 H, 2 × CH^A=CH^B), 6.96 (br s, Δν_{1/2} = 26.2 Hz, 2 H, 2 × CH^A=CH^B), 7.40–7.80 (br m, 6 H, Ar-H, Dipp). Spectra of **3** exhibit sharper signals in benzene-*d*₆ (400.13 MHz, benzene-*d*₆, 298 K): δ = 1.06 (d, ³J(H,H) = 6.30 Hz, 12 H, 2 × CH(CH₃)₂), 1.48 (d, ³J(H,H) = 6.30 Hz, 12 H, 2 × CH(CH₃)₂), 2.68 (s, 3 H, 1 × CH₃, η⁶-toluene), 3.44 (br m, 4 H, 4 × CH(CH₃)₂), 3.60 (br, 2 H, Ar-H, η⁶-toluene), 4.37 (s, 4 H, 1 × NCH₂N + 2 × Ar-H, η⁶-toluene), 5.55 (s, 1 H, Ar-H, η⁶-toluene), 6.19 (s, 4 H, 2 × CH^A=CH^B), 7.40 – 7.80 (br m, 6 H, Ar-H, Dipp). ¹³C{¹H} NMR (100.61 MHz, cyclohexane-*d*₁₂, 298 K): δ = 23.5 (s, 4 × CH(CH₃)₂), 25.0 (s, 1 × CH₃, η⁶-toluene), 29.0 (s, 4 × CH(CH₃)₂), 60.3 (s, 1 × NCH₂N), 74.2 (s, Ar-C, η⁶-toluene), 77.4 (s, C⁴, η⁶-toluene), 77.7 (s, Ar-C, η⁶-toluene), 77.9 (s, C¹, η⁶-toluene), 115.7 (s, 2 × CH^A=CH^B), 123.4 (s, 2 × CH^A=CH^B), 124.2 (s, 2 × C^{3,5}-H, Dipp), 129.1 (s, 2 × C⁴-H, Dipp), 140.9 (s, 2 × C¹, Dipp), 148.2 (s, 2 × C^{2,6}, Dipp), 198.4 (s, 2 × NC:N). ESI-MS (THF), *m/z*: calcd for [C₃₈H₄₈FeN₄]^{•+}: 616.3223. Found: 616.3240.

[Fe(D^{ipp}PC)₂(CH₂)₂(η⁶-C₆H₆)] (4**).** A Schlenk tube was charged with **1** (0.300 g, 0.504 mmol) and an excess of KC₈ (0.272 g, 2.015 mmol). A 1:1 (by volume) THF/benzene solution was added under rapid stirring to this solid mixture by cannula transfer at room temperature. After stirring at 6.5 h a dark-brown solution is noticed. The solvent was removed under reduced pressure and the remaining dark-brown residue extracted with hexane (50 mL). The color of the filtrate was light orange, and upon removal of solvent resulted in a mass of 15 mg (brown solid, product). The remaining reaction residue was then extracted with benzene (70 mL), and the dark-brown filtrate concentrated to dryness, revealing a dark-brown solid as product. Combined yield: 0.227 g (0.377 mmol, 75%). Crystals suitable for X-ray diffraction analysis were grown from a 1:6 (benzene: Et₂O) solution at 5 °C. ¹H NMR (200.13 MHz, benzene-*d*₆, 298 K): δ = 1.05 (br d, ³J(H,H) = 6.8 Hz, 12 H, 2 × CH(CH₃)₂), 1.44 (br d, ³J(H,H) = 6.7 Hz, 12 H, 2 × CH(CH₃)₂), 3.43 (br m, Δν_{1/2} = 21.3 Hz, 4 H, 4 × CH(CH₃)₂), 4.43 (br s, Δν_{1/2} = 3.8 Hz, 2 H, 1 × NCH₂N), 4.65 (br s, Δν_{1/2} = 3.24 Hz, 6 H, η⁶-benzene), 6.19 (br s, Δν_{1/2} = 3.2 Hz, 4 H, 2 × CH=CH^B), 7.15 (solvent signal + br s, 6 H, Ar-H, Dipp – cross peaks in 2D HMQC). ¹³C{¹H} NMR (50 MHz, benzene-*d*₆, 298 K): δ

= 22.8 (s, 2 × CH(CH₃)₂), 25.5 (s, 2 × CH(CH₃)₂), 28.3 (s, 4 × CH(CH₃)₂), 59.0 (signal located by HMQC as a cross peak to the signal at δ = 4.43 in ¹H NMR, 1 × NCH₂N), 75.4 (s, 6 × CH, η^6 -benzene), 116.3 (s, 2 × CH^A=CH^B), 123.0 (s, 2 × CH^A=CH^B), 124.1 (s, 2 × C^{3,5}-H, Dipp), 129.1 (s, 2 × C⁴-H, Dipp), 140.3 (s, 2 × C¹, Dipp), 147.7 (s, 2 × C^{2,6}, Dipp), 197.5 (s, 2 × NC:N, located by a weak cross peak with the CH=CH resonance in the 2D HMBC spectrum). ESI-MS (THF), *m/z*: calcd for [C₃₇H₄₆FeN₄ + H]⁺: 603.3145. Found: 603.3150. ⁵⁷Fe Mössbauer 80 K: δ = 0.43 mm·s⁻¹; ΔE_Q = 1.37 mm·s⁻¹.

[Fe(^{Dipp}C₂CH₂)(CO)₃] (6). A small Schlenk tube was charged with **3** (50 mg, 0.081 mmol) and Et₂O (5 mL) and stirred at room temperature as a dark-brown solution. The solution was frozen and degassed via a freeze–pump–thaw cycle and left under static vacuum. CO was introduced to the vessel at 1.2 atm pressure, and the vessel closed off. After ~1 min a color change to bright yellow was observed. All volatiles were removed in vacuo, and the remaining yellow solid dried for 0.5 h at room temperature. Yield: 0.045 g, (0.074 mmol, 91%). Repeated attempts at growing crystals for X-ray analysis were unsuccessful, in various solvents and under various conditions. ¹H NMR (200.13 MHz, benzene-*d*₆, 298 K): δ = 1.04 (br d, ³J(H,H) = 6.7 Hz, 12 H, 2 × CH(CH₃)₂), 1.42 (br d, ³J(H,H) = 6.7 Hz, 12 H, 2 × CH(CH₃)₂), 2.83 (ps sept, ³J(H,H) = 6.7 Hz, 4 H, 4 × CH(CH₃)₂), 4.68 (br s, $\Delta\nu_{1/2}$ = 22.4 Hz, 2 H, 1 × NCH₂N), 6.30 (br s, 2 H, 2 × CH^A=CH^B), 6.41 (br s, $\Delta\nu_{1/2}$ = 7.4 Hz, 2 H, 2 × CH^A=CH^B), 6.94–7.40 (solvent signal + m, 6 H, Ar-H, Dipp – cross peaks in 2D HMQC). ¹³C{¹H} NMR (50 MHz, benzene-*d*₆, 298 K): δ = 22.0 (s, 2 × CH(CH₃)₂), 25.6 (s, 2 × CH(CH₃)₂), 28.7 (s, 4 × CH(CH₃)₂), (not visible: 1 × NCH₂N), 123.8 (s, 2 × CH^A=CH^B), 124.2 (s, 2 × CH^A=CH^B), 124.4 (s, 2 × C^{3,5}-H, Dipp), 130.3 (s, 2 × C⁴-H, Dipp), 137.1 (s, 2 × C¹, Dipp), 146.7 (s, 2 × C^{2,6}, Dipp), 204.2 (s, 2 × NC:N), 222.9 (3 × CO). ESI-MS (THF), *m/z*: calcd for [C₃₄H₄₀FeN₄O₃ + H]⁺: 609.2523. Found: 609.2515; calcd for [C₃₃H₄₀FeN₄O₂ + H]⁺: 581.2573. Found: 581.2564 [M – CO + H]⁺; calcd for [C₃₂H₄₀FeN₄O + H]⁺: 553.2624. Found: 553.2615 [M – 2CO + H]⁺; calcd for [C₃₁H₄₀FeN₄ + H]⁺: 525.2675. Found: 525.2669 [M – 3 CO + H]⁺. ν (CO, cm⁻¹): 1968, 1890, 1865 (benzene solution).

Thermal conversion of 3 to 4-*d*₆. In a sealed NMR tube, **3** was dissolved in C₆D₆ and heated at 70 °C in an oil bath. The progress of the reaction was followed by NMR spectroscopy (¹H), where progressive conversion to **4-*d*₆** was observed, with concomitant liberation of free toluene. Only after 24 h of heating was the reaction complete. In addition, a ¹³C NMR spectrum was recorded at this time, which corresponded to **4-*d*₆** with toluene (free) and showed complete consumption of **3**. The ¹H and ¹³C NMR spectra match those of **4-*d*₆** generated by thermal means from **2** (vide supra) and contain signals corresponding to free toluene.

Procedure for the Reduction of Organic Amides. In a glovebox a Schlenk flask was charged with complex **4** (0.01 mmol, 1.0 mol %), the corresponding amide (**9a–d**) (1.0 mmol), and THF (2.0 mL). The flask was removed from the glovebox, and Ph₂SiH₂ (3.0 mmol) was added by syringe. The reaction mixture was stirred in a preheated oil bath at 70 °C for 24 h. The mixture was cooled in an ice bath and was treated with dodecane (100 μ L) as GC standard (for GC analysis) and aqueous sodium hydroxide solution (1.0 mL) with stirring. The reaction mixture was stirred for 60 min at room temperature and was then extracted with diethyl ether (2 × 10.0 mL). The combined organic layers were washed with brine, dried with anhydrous Na₂SO₄, and filtered. *n*-Dodecane (internal standard) was added, and an aliquot was removed for GC analysis (30 m Rxi-5 ms column, 40–300 °C). Furthermore, the analytical properties of the products are in accordance to commercially available authentic samples. **9a**: MS (EI) *m/z* 135 (38, M+), 91 (44), 65 (12), 58 (100). **9b**: MS (EI) *m/z* 164 (100, M+), 122 (29), 109 (57), 95 (30). **9c**: MS (EI) *m/z* 147 (100, M+), 117 (61). **9d**: MS (EI) *m/z* 223 (70, M+), 208 (100), 193 (66).

Theoretical Calculations. DFT calculations of complexes **2–4** (including **2'**) were performed at B3LYP level using 6-31G basis sets

of the GAUSSIAN 03 program package. Optimized structure of model compounds were obtained without symmetry constraints.

■ ASSOCIATED CONTENT

Supporting Information

Details on X-ray crystal structure analyses of **2–4**, selected NMR and HR-ESI-MS spectra of **1–6** as well as additional data on the catalytic procedures involving **4** and the Cartesian coordinates, NBO analyses, optimized structures, and additional MOs of **2–4** are available. This material is available free of charge via the Internet at <http://pubs.acs.org>.

■ AUTHOR INFORMATION

Corresponding Author

matthias.driess@tu-berlin.de

Notes

The authors declare no competing financial interest.

■ ACKNOWLEDGMENTS

The authors thank the Cluster of Excellence UniCat (financed by the Deutsche Forschungsgemeinschaft and administered by the TU Berlin) and the Sofja Kovalevskaja Program (financed by the Alexander von Humboldt Foundation) for financial support. We also express thanks to Dr. M. Schlangen for useful discussions concerning the HRMS spectra and Dr. E. Bill for recording the Mössbauer spectra of **1** and **4**. Dr. Elisabeth Irran is acknowledged for solving the X-ray structure of compound **2**.

■ REFERENCES

- (1) (a) Arduengo, A. J., III; Harlow, R. L.; Kline, M. *J. Am. Chem. Soc.* **1991**, *113*, 361. (b) Arduengo, A. J., III; Kline, M.; Calabrese, J. C.; Davidson, F. *J. Am. Chem. Soc.* **1991**, *113*, 9704.
- (2) See as examples: (a) Hock, S. J.; Schaper, L.-A.; Hermann, W. A.; Kühn, F. E. *Chem. Soc. Rev.* **2013**, *42*, 5073. (b) Folger, E.; Balaraman, E.; Ben-David, Y.; Leitens, G.; Shimon, L. J. W.; Milstein, D. *Organometallics* **2011**, *30*, 3826. (c) Schuster, O.; Yang, L.; Raubenheimer, H. G.; Albrecht, M. *Chem. Rev.* **2009**, *109*, 3445. (d) McGuinness, D. S.; Gibson, V. C.; Steed, J. W. *Organometallics* **2004**, *23*, 6288. (e) Hermann, W. A. *Angew. Chem., Int. Ed.* **2002**, *41*, 1290. (f) Hermann, W. A.; Weskamp, T.; Böhm, V. P. W. *Adv. Organomet. Chem.* **2001**, *48*, 1. (g) Bourissou, D.; Guerret, O.; Gabbai, F. P.; Bertrand, G. *Chem. Rev.* **2000**, *100*, 39.
- (3) For a concise overview see: Ingleson, M. J.; Layfield, R. A. *Chem. Commun.* **2012**, *48*, 3579.
- (4) Li, H.; Castro, L. C.; Zheng, J.; Roisnel, T.; Dorcet, V.; Sortais, J.-B.; Darcel, C. *Angew. Chem., Int. Ed.* **2013**, *52*, 8045.
- (5) Hatanaka, T.; Ohki, Y.; Tatsumi, K. *Chem.–Asian J.* **2010**, *5*, 1657.
- (6) Castro, L. C.; Sortais, J. B.; Darcel, C. *Chem. Commun.* **2012**, *48*, 151.
- (7) Meyer, S.; Orben, C. M.; Demeshko, S.; Dechert, S.; Meyer, F. *Organometallics* **2011**, *30*, 6692.
- (8) Zlatogorsky, S.; Muryn, C. A.; Tuna, F.; Evans, D. J.; Ingleson, M. J. *Organometallics* **2011**, *30*, 4974.
- (9) (a) Danopoulos, A. A.; Pugh, D.; Smith, H.; Saßmannshausen, J. *Chem.–Eur. J.* **2009**, *15*, 5491. (b) Danopoulos, A. A.; Wright, J. A.; Motherwell, W. B. *Chem. Commun.* **2005**, 784.
- (10) Liu, B.; Xia, Q.; Chen, W. *Angew. Chem., Int. Ed.* **2009**, *48*, 5513.
- (11) Zlatogorsky, S.; Ingleson, M. J. *Dalton Trans.* **2012**, *41*, 2685.
- (12) For a recent procedure, see: Huffer, A.; Jeffery, B.; Waller, B. J.; Danopoulos, A. A. *R. Chim.* **2013**, *16*, 557.
- (13) (a) Xiong, Y.; Yao, S.; Inoue, S.; Epping, J. D.; Driess, M. *Angew. Chem., Int. Ed.* **2013**, *52*, 7147. (b) Xiong, Y.; Yao, S.; Tan, G.; Inoue, S.; Driess, M. *J. Am. Chem. Soc.* **2013**, *135*, 5004.
- (14) Blom, B.; Enthaler, S.; Inoue, S.; Irran, E.; Driess, M. *J. Am. Chem. Soc.* **2013**, *135*, 6703.

(15) Another example of an 18 VE Fe(0) complex, stabilized by chelating phosphanes bearing an N₂ ligand which is easily eliminated is [Fe(depe)₂(η¹-N₂)] (depe = 1,2-bis(diethylphosphino)ethane; Komiyama, S.; Akita, M.; Yoza, A.; Kasuga, N.; Fukuoka, A.; Kai, Y. *J. Chem. Soc., Chem. Commun.* **1993**, 787.

(16) (a) For several examples where PMe₃ elimination from the complex [Fe(dmpe)₂(PMe₃)] (dmpe = 1,2-bis(dimethylphosphino)ethane) enables access to a variety of Fe(0) complexes, see: Blom, B., Ph.D. Thesis, University of Bonn, Cuvillier Verlag, Göttingen, 2011 (b) Ref 14.

(17) Recently theoretical calculations have been reported for the complex [Fe{=PH}(NHC)(η⁶-C₆H₆)] probing the possible stabilization of phosphinidene fragments by "Fe(NHC)(η⁶-C₆H₆)", see: Aktas, H.; Slootweg, J. C.; Ehlers, A. W.; Lutz, M.; Spek, A. L.; Lammertsma, K. *Organometallics* **2009**, 28, 5166.

(18) In fact, the only other example of any iron complex bearing mutually an NHC and PMe₃ ligand is the Fe(0) complex [Fe(C,N,C)(η¹-N₂)(PMe₃)] (C,N,C = tridentate NHC ligand with pyridyl group); ref 9b.

(19) For other Fe complexes bearing mutually NHC and other phosphane ligands see as examples: (a) Yu, I.; Wallis, C. J.; Patrick, B. O.; Diaconescu, P. L.; Mehrkhodavandi, P. *Organometallics* **2010**, 29, 6065. (b) Hitchcock, P. B.; Lappert, M. F.; Thomas, S. A.; Thorne, A. J.; Carty, A. J.; Taylor, N. J. *J. Organomet. Chem.* **1986**, 315, 27. (c) Lappert, M. F.; Pye, P. L. *J. Chem. Soc., Dalton Trans.* **1977**, 2172. (d) Lappert, M. F.; MacQuitty, J. J.; Pye, P. L. *J. Chem. Soc. Chem. Commun.* **1977**, 411.

(20) Rathke, J. W.; Muetterties, E. L. *J. Am. Chem. Soc.* **1975**, 97, 3272.

(21) (a) Similar phenomena have been observed in the case of [FeH(PMe₃)₃(η²-PMe₂CH₂)], which when reacted with a group that inserts into the Fe-C bond of the η²-PMe₂CH₂ ligand also affords a mixture of stereoisomers. See ref 16. (b) A further stereoisomer is also possible for [FeH{(D¹PPC)₂CH₂}(PMe₃)(η²-PMe₂CH₂)] with H and the CH₂ of η²-PMe₂CH₂ mutually trans, and the PMe₂ of η²-PMe₂CH₂ and PMe₃ mutually cis with respect to each other and the latter both trans to the {(D¹PPC)₂CH₂} group. This arrangement is however unlikely and excluded since H and CH₂ are strong trans ligands. The assignment of the other stereoisomers was made on the basis of the ²J(H_AP_a) and ²J(H_BP_b) coupling constants as well as the ²J(P_aP_b) coupling constants for each stereoisomer.

(22) For a good explanation of NMR time scale and dynamic processes see: Bryant, R. G. *J. Chem. Educ.* **1983**, 60, 933.

(23) The Supporting Information contains a selection of NMR spectra for 1–6, ESI-MS spectra for 2–6, details of the DFT calculations (including optimized structures of complexes 2, 2', 3, and 4) and details concerning the X-ray structural elucidation of 3 and 4.

(24) William-Smith, D. L.; Wolf, L. R.; Skell, P. S. *J. Am. Chem. Soc.* **1972**, 94, 4042.

(25) Green, M. L. H.; Wong, L.-L. *J. Chem. Soc. Chem Commun.* **1984**, 1142.

(26) (a) Ittel, S. D.; Tolman, C. A. *Organometallics* **1982**, 1, 1432. (b) Middleton, R.; Hull, J. R.; Simpson, S. R.; Tomlinson, C. H.; Timms, P. L. *J. Chem. Soc. Dalton* **1973**, 120.

(27) Hermes, A. R.; Warren, T. H.; Girolami, G. S. *J. Chem. Soc., Dalton Trans.* **1995**, 301.

(28) This is in fact the only structurally characterized complex of the type [Fe(η⁶-arene)(P₂)] (P₂ = chelating ligand), see: Kubo, H.; Hirano, M.; Komiyama, S. *J. Organomet. Chem.* **1998**, 556, 89. Surprisingly, no examples of structurally characterized complexes of the type [Fe(η⁶-arene)(PR₃)₂] (i.e., with two monodentate phosphane ligands) exists, even though they have been known since the early 1970s, see: William-Smith, D. L.; Wolf, L. R.; Skell, P. S. *J. Am. Chem. Soc.* **1972**, 94, 4042.

(29) Schnöckelborg, E.; Khusniyarov, M. M.; de Bruin, B.; Hartl, F.; Langer, T.; Eul, M.; Schulz, S.; Pöttgen, R.; Wolf, R. *Inorg. Chem.* **2012**, 51, 6719.

(30) (a) Bart, S. C.; Hawrelak, E. J.; Lobkovsky, E.; Chirik, P. J. *Organometallics* **2005**, 24, 5518. (b) Archer, A. M.; Bouwkamp, M. W.;

Cortez, M.-P.; Lobkovsky, E.; Chirik, P. J. *Organometallics* **2006**, 25, 4269.

(31) Radonovich, L. J.; Eyring, M. W.; Groshens, T. J.; Klabunde, K. J. *J. Am. Chem. Soc.* **1982**, 104, 2816 The authors claim in this paper the preparation of a 2,2'-bipy Fe(0) complex, which could be clearly disproven by Wieghardt and Scarborough; see ref 32.

(32) Scarborough, C. C.; Wieghardt, K. *Inorg. Chem.* **2011**, 50, 9773.

(33) The X-ray structure of Fe(CO)₂{η⁶-p-MeC₆H₄C(OSiMe₃)(C₈H₁₂)} exists as the only other example of a structurally characterized complex of the motif Fe(arene)L₂ (L = any heteroatom). Although it is tempting to consider this a genuine Fe(0) complex, no Mössbauer spectrum was recorded nor DFT studies carried out, so the role of the substituent on the coordinated arene ring: C(OSiMe₃)(C₈H₁₂) in potentially rendering the arene redox active, can also not be excluded completely. See: Chen, J.; Yin, J.; Fan, Z.; Xu, W. *J. Chem. Soc., Dalton Trans.* **1988**, 2903.

(34) See as good examples: (a) Sosinsky, B. A.; Norem, N.; Shong, R. *Inorg. Chem.* **1982**, 21, 4229. (b) Sosinsky, B. A.; Shelly, J.; Shong, R. *Inorg. Chem.* **1981**, 20, 1370. (c) Carroll, W. E.; Deeney, F. A.; Delaney, J. A.; Lalor, F. J. *J. Chem. Soc., Dalton Trans.* **1973**, 718. (d) Collins, R. L.; Pettit, R. J. *Chem. Phys.* **1963**, 39, 3433.

(35) Even the simple Bancroft point-charge model can be used, to an extent, to interpret such systems, see as examples: (a) Bancroft, G. M.; Libbey, E. T. *J. Chem. Soc., Dalton Trans.* **1973**, 2103. (b) Bancroft, G. M.; Mays, M. J.; Prater, B. E. *J. Chem. Soc. A* **1970**, 956. (c) Bancroft, G. M.; Mays, M. J.; Prater, B. E.; Stefanini, F. P. *J. Chem. Soc. A* **1970**, 2146.

(36) Ref 16 contains the ⁵⁷Fe Mössbauer spectra of these complexes with a full discussion on their δ and ΔE_Q parameters, along with quantum chemical calculations elucidating the effect of changing the geometry from SQPY to TBPY and the effect this has on the ΔE_Q parameter, whereby an increase is observed.

(37) Basis sets employed: B3LYP/6-31G* for all atoms. Performed using Gaussian 03, revision E.01. See Supporting Information for more full details concerning the DFT calculations of 3 and 4.

(38) As a good example of this see: Lavallo, V.; Grubbs, R. H. *Science* **2009**, 326, 559.

(39) We also investigated the reaction of 3 with CH₃I, which affords a yellow, and according to NMR spectra, a highly paramagnetic complex, most likely [Fe{(D¹PPC)₂CH₂}(CH₃)I] (5) which resembles the spectra of the Fe(II) precursor, 1 (high-spin (S = 2) tetrahedral complex). A fitting ESI-MS of the [M – I]⁺ signal confirms the proposed composition of 5. Several attempts to obtain crystals suitable for X-ray diffraction analysis to confirm the structure of 5 were unsuccessful, and so we leave this complex out of the main discussion. Here the synthesis: A small Schlenk tube was charged with 3 (50 mg, 0.081 mmol) and Et₂O (5 mL) and stirred at room temperature as a dark brown solution. An excess of MeI was added at room temperature via syringe (0.5 mL). An immediate color change to bright yellow was observed. All volatiles were removed in vacuo and the remaining yellow solid dried for 0.5 h at room temperature. Yield: 0.052 g, (0.078 mmol, 96%). Repeated attempts at growing crystals for X-ray analysis were unsuccessful, in various solvents and under various conditions. ¹H NMR (200.13 MHz, benzene-d₆, 298K): δ = –8.18 (v br), –4.38 (v br, Δν_{1/2} = 161.8 Hz), –2.66 (v br, Δν_{1/2} = 31.4 Hz), –1.10 (v br, Δν_{1/2} = 30.5 Hz), 0.23 (br, Δν_{1/2} = 9.0 Hz), 1.05 (br m), 2.05 (br, Δν_{1/2} = 8.2 Hz), 27.70 (v br, Δν_{1/2} = 238.9 Hz), 30.68 (v br, Δν_{1/2} = 98.9 Hz), 55.86 (v br), 63.2 (v br, Δν_{1/2} = 52.0 Hz). ESI-MS (THF), m/z: calcd for [C₃₂H₄₃FeN₄I – I]⁺: 539.2832. Found: 539.2824.

(40) As a recent example of a very facile toluene/C₆D₆ exchange from a low-valent Ni system from our group, see: Meltzer, A.; Präsaang, C.; Milsmann, C.; Driess, M. *Angew. Chem., Int. Ed. Engl.* **2009**, 48, 3170.

(41) See as examples: (a) Bezier, D.; Sortais, J.-B.; Darcel, C. *Adv. Synth. Catal.* **2013**, 355, 19. (b) Darwish, M.; Wills, M. *Catal. Sci. Technol.* **2012**, 2, 243. (c) Nakazawa, H.; Itazaki, M. *Topi. Organomet. Chem.* **2011**, 33, 27. (d) aAddis, D.; Das, S.; Junge, K.; Beller, M. *Angew. Chem., Int. Ed.* **2011**, 50, 6004. (e) Junge, K.; Schröder, K.; Beller, M. *Chem. Commun.* **2011**, 47, 4849. (f) Zhang, M.; Zhang, A.

Appl. Organomet. Chem. **2010**, *24*, 751. (g) Das, S.; Zhou, S.; Addis, D.; Enthaler, S.; Junge, K.; Beller, M. *Top. Catal.* **2010**, *53*, 979. (h) Morris, R. H. *Chem. Soc. Rev.* **2009**, *38*, 2282. (i) Czaplik, W. M.; Mayer, M.; Cvengros, J.; Jacobi von Wangelin, A. *ChemSusChem* **2009**, *2*, 396. (j) *Iron Catalysis in Organic Chemistry*; Plietker, B., Ed.; Wiley-VCH: Weinheim, Germany, 2008. (k) Gaillard, S.; Renaud, J.-L. *ChemSusChem* **2008**, *1*, 505. (l) Correa, A.; Mancheño, O. G.; Bolm, C. *Chem. Soc. Rev.* **2008**, *37*, 1108. (m) Sherry, B. D.; Fürstner, A. *Acc. Chem. Res.* **2008**, *41*, 1500. (n) Enthaler, S.; Junge, K.; Beller, M. *Angew. Chem., Int. Ed.* **2008**, *47*, 3317. (o) Bullock, R. M. *Angew. Chem.* **2007**, *119*, 7504; *Angew. Chem., Int. Ed.* **2007**, *46*, 7360. (p) Bolm, C.; Legros, J.; Le Pailh, J.; Zani, L. *Chem. Rev.* **2004**, *104*, 6217. (q) Bauer, E. B. *Curr. Org. Synth.* **2008**, *12*, 1341.

(42) (a) Warratz, S.; Postigo, L.; Royo, B. *Organometallics* **2013**, *32*, 893. (b) Volkov, A.; Buitrago, E.; Adolfsson, H. *Eur. J. Org. Chem.* **2013**, 2066. (c) Das, S.; Wendt, B.; Moeller, K.; Junge, K.; Beller, M. *Angew. Chem., Int. Ed.* **2012**, *51*, 1662. (d) Bezier, D.; Venkanna, G. T.; Sortais, J.-B.; Darcel, C. *ChemCatChem* **2011**, *3*, 1747. (e) Tsutsumi, H.; Sunada, Y.; Nagashima, H. *Chem. Commun.* **2011**, *47*, 6581. (f) Sunada, Y.; Kawakami, H.; Imaoka, T.; Motoyama, Y.; Nagashima, H. *Angew. Chem., Int. Ed.* **2009**, *48*, 9511. (g) Zhou, S.; Junge, K.; Addis, D.; Das, S.; Beller, M. *Angew. Chem., Int. Ed.* **2009**, *48*, 9507.